XY chain with random anisotropy: Magnetization law, susceptibility, and correlation functions at $T=0$

Ronald Dickman and Eugene M. Chudnovsky
Department of Physics and Astronomy, Herbert H. Lehman College, City University of New York, Bronx, New York 10468
(Received 5 November 1990; revised manuscript received 23 April 1991)

The random-anisotropy model in one dimension, at zero temperature, is studied analytically and in Monte Carlo simulations, focusing on the magnetization curve as a function of disorder strength D, and on the susceptibility and correlation functions. The predicted scaling of the susceptibility (for weak disorder), $\chi \propto D^{-4/3}$, is verified, as is the prediction $|M-1| \propto H^{-3/2}$ on approaching saturation. The correlation length does not follow the expected behavior, $R_f \propto D^{-2/3}$. Nonequilibrium effects are evident: Hysteresis persists even for small disorder, and (steady-state) correlation functions depend strongly upon the initial state of the system. A new simulation method is introduced, which is more effective than the usual Metropolis algorithm for weak disorder.

I. INTRODUCTION

Experiments on amorphous ferromagnets have revealed a number of systems whose properties are well described by the random-anisotropy model.[1–4] In particular, it yields correct predictions for spin-spin correlation functions, the susceptibility, and the magnetization law.[2–6] This model has attracted considerable interest, in both the strong- and weak-anisotropy limits.[1–16] Since neither of these limits has been solved rigorously, some important questions remain unanswered. Among them are the range of validity of the continuous-spin-field approximation, the role of metastable states, and the sharpness of the transition from strong- to weak-anisotropy behavior. In the present work we examine various properties of the model, including the magnetization law and correlation functions, analytically, and in Monte Carlo simulations. For simplicity, we investigate a one-dimensional version of the model.

In this paper we present a detailed analytical and numerical study of a classical, one-dimensional, ferromagnetic, XY chain with random anisotropy, at zero temperature. The system is characterized by the Hamiltonian

$$E=-\sum_i [J\mathbf{S}_i\cdot\mathbf{S}_{i+1}+D(\hat{\mathbf{n}}_i\cdot\mathbf{S}_i)^2+\mathbf{H}\cdot\mathbf{S}_i] , \quad (1)$$

where $\mathbf{S}_i$ and $\hat{\mathbf{n}}_i$ ($|\mathbf{S}_i|^2=|\hat{\mathbf{n}}_i|^2=1$), are the spin and easy-axis vectors at site i. $J(>0)$ is the nearest-neighbor coupling, D is the anisotropy strength, and $\mathbf{H}$ is the magnetic field. The easy axes $\hat{\mathbf{n}}_i$ (representing frozen-in disorder) are uniformly and independently distributed on the unit circle. In the limit $D \gg J$, spins are oriented along the anisotropy axes, and one obtains an Ising model with random couplings and external fields, as investigated recently by Derrida and Zippelius.[17] When $D \ll J$, $\mathbf{S}$ is slowly varying, so that it is also useful to consider a continuous spin-field version of the model[2]

$$E=\int dx \left[\frac{\alpha}{2}|\nabla\mathbf{S}|^2-\frac{\beta}{2}(\hat{\mathbf{n}}\cdot\mathbf{S})^2-\mathbf{H}\cdot\mathbf{S} \right] , \quad (2)$$

where $\alpha \propto J, \beta \propto D$, and $\mathbf{S}(x)$ and $\hat{\mathbf{n}}(x)$ are, respectively, the spin and random-anisotropy fields.

Applying the usual prescription of statistical mechanics to this model at zero temperature, one would evaluate thermodynamic properties in the ground state for a given set of $\{\hat{\mathbf{n}}_i\}$, and then average over disorder. However, the ground-state configuration is inaccessible analytically and numerically, and is likely not relevant in many experiments on disordered materials at low temperatures. That is, the presence of many local energy minima, mutually inaccessible on laboratory timescales, causes the system to be generically in a metastable state, and gives rise to reproducible hysteresis effects. In the present study the emphasis is on properties of local minimum-energy configurations. The nature of this configuration often depends strongly upon the initial state.

The limit of weak anisotropy presents subtleties not encountered for strong disorder. While the spins remain correlated over large domains, it is known that random fields[9] and random anisotropy[11,12] destroy long-range order in systems with a continuous symmetry order parameter, for dimension $d \leq 4$. Even in the ground state, the local magnetization vector $\mathbf{S}$ describes a random walk under the influence of the disorder, so that, in the absence of an external magnetic field, $\mathbf{S}$ smoothly and stochastically rotates along the chain. In the presence of weak disorder, the ground state is characterized by a ferromagnetic correlation length R_f, the length over which $\mathbf{S}(x)$ exhibits a significant rotation. The correlation length is expected to scale[9] as $R_f \propto (J/D)^{2/(4-d)}$.

The low-temperature, weak-anisotropy regime of the model has been variously described as a "correlated spin glass" (CSG),[2] and as a ferromagnet with wandering axes (FWA).[8] Because of the long correlation lengths, simulations in the weak-anisotropy limit involve long relaxation times. We are aware of two previous simulation studies of the XY model with random anisotropy. The first is by Serota and Lee[18] who found (for a one-dimensional system) that the hysteresis and memory effects commonly associated with strong disorder also occur when $D \ll J$.

The second is a very recent study of the model in two dimensions by Dieny and Barbara.[19,20] Their work focuses on spin-spin correlations and the role of topological defects in the magnetization process.

In this paper we present a more detailed study of the model in one dimension. In Sec. II we derive analytical results for the magnetization on approaching saturation, and in the demagnetization process, and for correlation functions. We describe our Monte Carlo simulation methods in Sec. III, and present the results in Sec. IV. Section V contains a brief summary and discussion.

II. THEORY

A. Demagnetization

We begin our discussion with the demagnetization curve, in the strong-field limit. This is the simplest regime to understand, as the strong field dominates the random anisotropy, and renders the system essentially linear. We assume that H remains sufficiently large that $M \simeq 1$. It is convenient to describe the configuration in terms of θ_i, the angle between $\mathbf{S}_i$ and $\mathbf{H}$ (the latter is taken along the $+x$ direction), so that

$$E = -\sum_i [J\cos(\theta_i - \theta_{i-1}) + D\cos^2(\theta_i - \phi_i) + H\cos\theta_i] , \tag{3}$$

where ϕ_i is the angle between $\hat{\mathbf{n}}_i$ and $\mathbf{H}$. Local equilibrium requires that for each i

$$J[\sin(\theta_{i+1} - \theta_i) - \sin(\theta_i - \theta_{i-1})] - D\sin[2(\theta_i - \phi_i)] - H\sin\theta_i = 0 . \tag{4}$$

Since the θ_i are assumed small, $\sin\theta_i \cong \theta_i$, and Eq. (4) becomes

$$(\Delta^2 - p^2)\theta_i = -(D/J)\sin 2\phi_i , \tag{5}$$

where $\Delta^2\theta_i = \theta_{i+1} + \theta_{i-1} - 2\theta_i$, and $p^2 \equiv H/J$. The formal solution is

$$\theta_i = (D/J)\sum_j G_{ij}(p)\sin(2\phi_j) , \tag{6}$$

where the Green's function is

$$G_{ij}(p) = \frac{e^{-Q|i-j|}}{2(1-e^{-Q}) + p^2} \tag{7}$$

with $\cosh Q = 1 + p^2/2$. The (disorder-averaged) loss of magnetization, $\delta M = 1 - M = 1 - \langle \cos\theta_i \rangle$, is then

$$\delta M = (1/2)\langle \theta_i^2 \rangle = (1/2)(DA/J)^2 \sum_{j,k} e^{-Q(|i-j|+|i-k|)} \times \langle \sin(2\phi_{i-j})\sin(2\phi_{i-k}) \rangle , \tag{8}$$

where $A = [2(1-e^{-Q}) + p^2]^{-1}$. Using $\langle \sin(2\phi_j)\sin(2\phi_k) \rangle = \delta_{j,k}/2$, we have

$$\delta M = (DA/2J)^2 \sum_{j=-\infty}^{\infty} e^{-2Q|j|} = (DA/2J)^2 \coth Q = (D/4J)^2 \frac{1 + p^2/2}{p^3(1 + p^2/4)^{3/2}} . \tag{9}$$

Equation (9) is valid when the magnetic field is sufficiently large that $\delta M \ll 1$. For strong disorder, $(D/4J)^2 \gg 1$, this implies $2H \gg D$, and in this limit $\delta M = D^2/4H^2$, independent of J. In the case of weak disorder, $(D/4J)^2 \ll 1$, $\delta M \ll 1$ when $H \gg J(D/4J)^{4/3}$. When $J \gg H \gg J(D/4J)^{4/3}$, $\delta M \propto H^{-3/2}$, while for $J \ll H$, $\delta M = D^2/4H^2$, as in the strong-disorder case.

B. Spin-spin correlation function

In this section we present a heuristic argument for the spin-spin correlation function for weak anisotropy. Consider the correlation function for spin components $S_i^{\perp}$ *transverse* to the field:

$$\langle S_i^{\perp} S_j^{\perp} \rangle = \langle \sin\theta_i \sin\theta_j \rangle . \tag{10}$$

For the demagnetization regime studied in the previous section, $|\theta_i| \ll 1$, so that the right-hand side (rhs) of Eq. (10) reduces to $\langle \theta_i \theta_j \rangle$. Then using Eq. (6) we obtain

$$\langle S_i^{\perp} S_j^{\perp} \rangle = (D/J)^2 \sum_{n,m} G_{i,n}(p) G_{j,m}(p) \times \langle \sin(2\phi_n)\sin(2\phi_m) \rangle = 2(D/4J)^2 \frac{1 + p^2/2}{p^3(1 + p^2/4)^{3/2}} \times (1 + |i-j|\tanh Q) e^{-Q|i-j|} \tag{11}$$

with $\cosh Q = 1 + p^2/2$ as before.

When $i = j$, Eq. (11) is equivalent to Eq. (9). The two expressions share the same range of validity, viz., $p^3 \gg (D/4J)^2$. Let $\varepsilon^3 = (D/4J)^2$. When $\varepsilon \ll p \ll 1$, Eq. (11) becomes

$$\langle S_i^{\perp} S_j^{\perp} \rangle = (\varepsilon/p)^3 (1 + p|i-j|) e^{-p|i-j|} , \tag{12}$$

where $p^{-1} = (J/H)^{1/2} \gg 1$ is the transverse correlation length. Note that D appears only in the prefactor of Eq. (12), so that the *normalized* transverse correlation function $c_{\perp}(|i-j|) \equiv \langle S_i^{\perp} S_j^{\perp} \rangle / \langle (S_i^{\perp})^2 \rangle$ is independent of disorder strength. The validity of Eq. (12) fails when $p \lesssim \varepsilon$ ($H \lesssim \varepsilon^2 J$), at which point the transverse and longitudinal components of S are of comparable magnitude.

The evaluation of the full spin-spin correlation function for the random-anisotropy model remains an open problem, although the calculation is tractable in the mean spherical approximation. We show in the Appendix that this approximation yields (for $H = 0$) the following expression for the correlation function:

$$C(|i-j|) \equiv \langle \mathbf{S}(x_1) \cdot \mathbf{S}(x_2) \rangle = (1 + k|x_1 - x_2|) e^{-k|x_1 - x_2|} \tag{13}$$

with

$$k=\left[\frac{\beta^2 r}{8\alpha^2}\right]^{1/3}, \tag{14}$$

where r is the correlation length for the random axes $\hat{\mathbf{n}}_i$ (on the order of one lattice spacing). Equation (14) is in accord with the result of the Imry-Ma argument.[9]

C. Approach to saturation

To get an idea of how the magnetization behaves on approach to saturation, we first consider the model without disorder. In the continuous-space version of the model the spin field is described in terms of an angle $\theta(x)$, and the energy takes the form

$$E=\int dx\left[\frac{\alpha}{2}(d\theta/dx)^2-H\cos\theta\right]. \tag{15}$$

Extremal trajectories satisfy the time-independent sine-Gordon equation:

$$d^2\theta/dx^2=\frac{H}{\alpha}\sin\theta\ . \tag{16}$$

Equation (16) admits the well-known soliton solution

$$\theta(x)=4\tan^{-1}\{\exp[p(x-x_0)]\} \tag{17}$$

which corresponds to a rotation through (nearly) 2π over a distance $R(H)\simeq p^{-1}=(\alpha/H)^{1/2}$. At $x=x_0$ the spin is oriented opposite to the field. The low-lying configurations of the (nonrandom) sine-Gordon chain are a "gas" weakly interacting solitons or "kinks." In the present case, the kinks are a remnant of the initial condition. They may become pinned due to the random anisotropy. In any event, the system cannot relax to the kink-free ground state via local dynamics. With increasing field strength, however, the kinks shrink, and, in the discrete-space model, disappear when $p\approx 1$, i.e., when $H\approx J$. For large H the system contains compact kinks separated by essentially saturated regions. Each kink represents a magnetization "deficit" of

$$\int dx[1-\cos\theta(x)]=4/p\ , \tag{18}$$

where $\theta(x)$ is given by Eq. (17). If we let n be the number of kinks per unit length, then $\delta M\approx 4n/p$. As long as H is not large enough to destroy the kinks, n remains constant and $\delta M\propto H^{-1/2}$. We expect a more rapid approach to saturation when $H>J$, due to field-induced collapse of kinks.

D. Susceptibility

The prediction that for $D\ll J$, the zero-field susceptibility scales as

$$\chi\propto(J/D)^{4/(4-d)} \tag{19}$$

in random-anisotropy systems has been obtained by three groups of authors[5–7] using different arguments. This prediction is in good agreement with the experimental result,[20] $\chi\propto(J/D)^{3.8\pm0.2}$ for three-dimensional amorphous ferromagnets. For $d=1$, Eq. (19) gives $\chi\propto D^{-4/3}$. A simple interpretation of this result is as follows. According to Eq. (9) the saturation knee ($M\simeq 1$) occurs at $H=H_k\approx J(D/4J)^{4/3}$. One may expect, therefore, that $\chi\propto 1/H_k\propto D^{-4/3}$, in the presence of weak disorder.

In summary, we have presented simple theoretical arguments for the correlation function (in zero field), and for the magnetization approaching and departing from saturation. The predictions are compared with simulation results in Sec. IV.

III. SIMULATION METHODS

The system consists of L sites ($L=1000$ or 2000), with periodic boundary conditions. The nearest-neighbor interaction parameter J is set to unity, so the system is characterized simply by D (disorder strength) and H (external field). Associated with each site is a spin variable θ_i and an easy axis ϕ_i. The latter are uniformly and independently distributed on $[0,2\pi]$. For a particular realization or "sample," the ϕ_i are held constant while the spins evolve toward a (local) minimum-energy configuration.

Two simulation algorithms, both involving only single-spin dynamics, were employed. The first is an implementation of the standard Metropolis algorithm at zero temperature. At each step of the evolution, a site j is chosen at random and the spin θ_j is subject to a random displacement $\theta_j\rightarrow\theta_j'=\theta_j+\xi$, where ξ is a random number uniform on $[-d,d]$. θ_j is replaced with θ_j' if the attendant change in energy is less than or equal to zero; otherwise θ_j is retained. The scale of the random displacement d is reduced during the course of the simulation, so as to maintain an acceptance rate of about 25%.

The "pure Metropolis" algorithm described above is not useful for $D<0.1$, due to the very long time required for each spin to reach its (local) minimum-energy orientation. Relaxation would be faster if the trial spin value θ_i were set to minimize the energy, given $\theta_{i-1},\theta_{i+1},\phi_i$, and H. Since the energy is a fairly complicated function, it is more efficient to *estimate* the energy-minimizing θ_i using Newton's method. [To avoid the well-known instability associated with Newton's method, the condition $E(\theta_i')<E(\theta_i)$ is verified prior to accepting the trial spin value.] There is little point iterating the process at a given site, as a change in one spin necessitates a change in its neighbors. Instead, the process is repeated at another randomly chosen site. Compared with the Metropolis algorithm, our application of Newton's method yields a more rapid approach to a local energy minimum, but is less likely to discover deeper energy minima nearby. For this reason we adopted a *hybrid* algorithm, in which "Newton" and "Metropolis" steps alternate. The hybrid algorithm was employed in all studies with $D<0.1$. A comparison of results obtained with the two methods is presented in the following section.

The initial stage of the simulation is typically an ultrafast quench from a disordered state to $T=0$, with no applied magnetic field. The system therefore settles into a local minimum-energy configuration. We regard the system as effectively relaxed into a steady state when the magnetization changes by less than 10^{-4} over a period of

10^5 trials (for $D \leq 0.1$, this period was extended to 10^7 trials). The various contributions to the energy reach steady values before the magnetization does. Once a steady state was attained, subsequent points along the magnetization curve were obtained by making an incremental change in the applied field, and allowing the configuration to evolve to a new steady state.

IV. SIMULATION RESULTS

A. Configurations

We begin with a qualitative discussion of typical spin configurations. To convey the overall organization of the system (with 1000–2000 spins) we employ a toroidal representation, in which the azimuthal angle corresponds to x (with periodic boundary conditions), and spin orientation is represented by the toroidal angle. Figure 1 shows typical configurations in the absence of an external magnetic field. For very weak disorder ($D=0.02$) the spin direction varies quite smoothly; for $D=0.2$ many more kinks are evident. Figure 2 illustrates the disappearance of kinks with increasing field strength H. At intermediate H values the configuration exhibits two kinds of structure: an erratic, small-amplitude meander in response to the random anisotropy, and occasional kinks, which represent a remnant of the initial state. (All memory of the initial configuration is of course erased upon saturation.)

B. Hysteresis

A hallmark of the importance of metastability, and of the inaccessibility of the ground state, is hysteresis. The initial magnetization curves and hysteresis loops observed in simulations at D values of 1, 0.5, and 0.1, are displayed in Figs. 3, 4, and 5, respectively. As expected, the extent of the loop increases with D. Hysteresis is clearly present even when $D=0.1$, and it is reasonable to expect it to persist in the presence of arbitrarily small disorder. In Figs. 4 and 5 the hysteresis loops observed using different simulation algorithms (pure Metropolis and Newton's-method–Monte Carlo hybrid) are compared. For $D=0.5$ the curves are essentially identical, but for $D=0.1$ the loop obtained with the hybrid method is distinctly smaller. Thus, in the case of weak disorder, differences in the dynamics may affect the details of the magnetization curve, but not its basic features. Hysteresis appears to be an intrinsic property of the disordered system evolving via local dynamics, as it is observed with either algorithm. Also of note are the discontinuities evident in the $D=0.1$ magnetization curves.

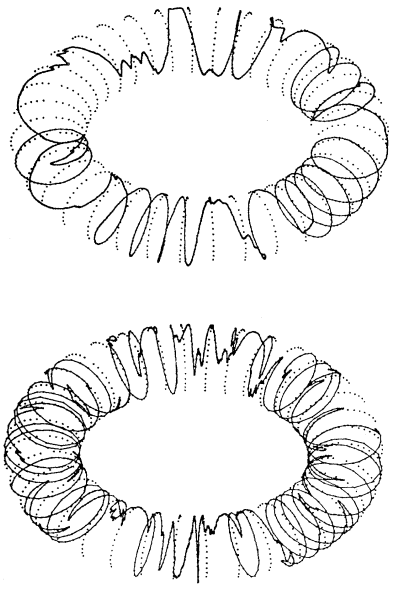

FIG. 1. Typical zero-field, steady-state spin configurations. In this diagram the position on the large circle represents the x coordinate, while that on the small circle represents the spin orientation $\theta(x)$. Upper: $D=0.02$; lower: $D=0.2$.

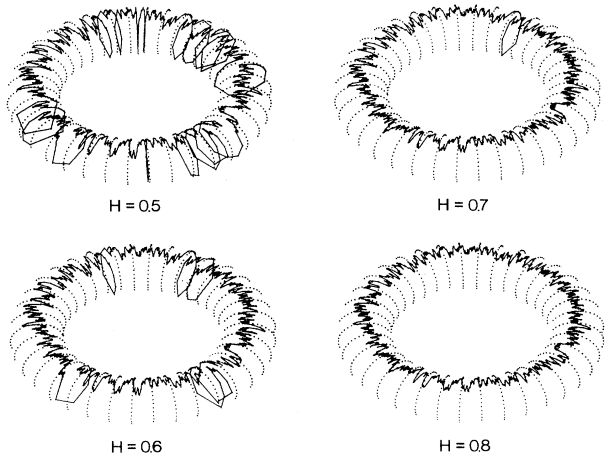

FIG. 2. Evolution of the steady-state configuration under an increasing external field H. The disorder strength $D=0.5$.

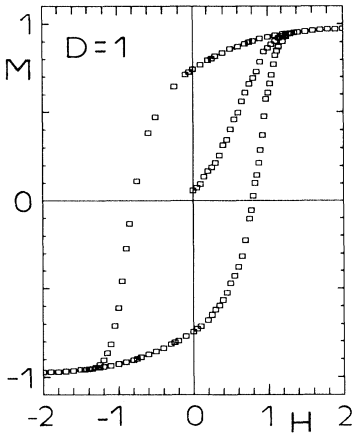

FIG. 3. Magnetization curve, $D=1.0$.

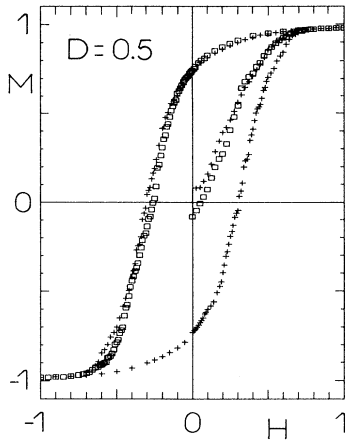

FIG. 4. Magnetization curve, $D=0.5$. +: pure Metropolis algorithm; squares: hybrid algorithm.

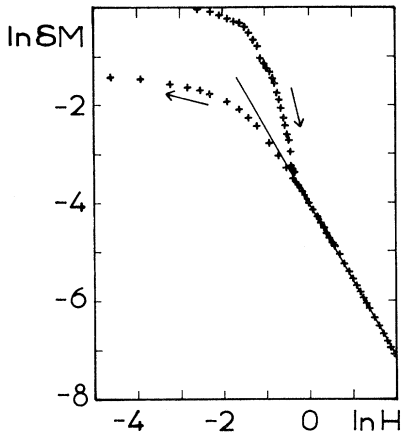

FIG. 6. Detail of magnetization curve, $D=0.5$. The slope of the straight line is -1.57.

Their presence suggests that the weakly disordered system can be trapped in a local energy minimum.

C. Demagnetization and saturation

A more detailed examination of the magnetization curve near saturation is shown in Figs. 6 and 7, for $D=0.5$ and 0.1, respectively. In both cases we find some support for the power law: $M \propto H^{-3/2}$, along the demagnetization curve, derived in Sec. II A. No evidence for the scaling $M \propto H^{-2}$ (expected to apply for $H \gg J$), is found. Such behavior cannot be ruled out for larger fields than were investigated, i.e., in the range $\delta M < 10^{-3}$. Finally, the data on approach to saturation shown in Fig. 6 give no clear evidence for the prediction $M \propto H^{-1/2}$.

D. Correlation functions

We have determined the spin-spin correlation function (at $H=0$) for anisotropy strength D ranging from 0.05 to 0.9. Typical results are shown in Figs. 8 and 9, for $D=0.05$ and 0.1, respectively. These plots represent averages over five different samples, which were allowed to relax from a random initial configuration. Evidently the correlation function of Eq. (13) (the result of the mean-spherical approximation), can be fit to the data *provided the correlation length k^{-1} is adjusted.* The continuous curves in Figs. 8 and 9 represent Eq. (13) with k determined not by Eq. (14) (which yields a sizable overestimate for the correlation length), but rather from a least-squares fit to the first 20 data points. While the data do not provide a compelling justification for Eq. (13), we note that the points cannot be fit very well by an exponential or a Gaussian. The prediction $k \propto D^{-2/3}$ is not supported by the simulation results, which instead suggest $k \propto D^{-0.46}$ (see Fig. 10).

The disagreement between Eq. (14) and the simulation results for the correlation length may reflect the inade-

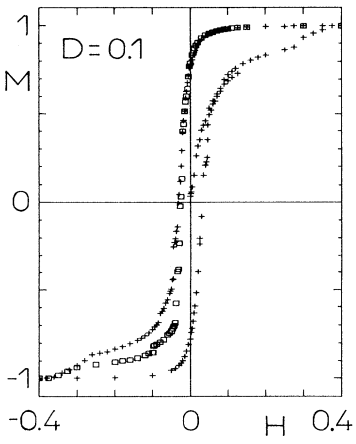

FIG. 5. Magnetization curve, $D=0.1$. Symbols as in Fig. 4.

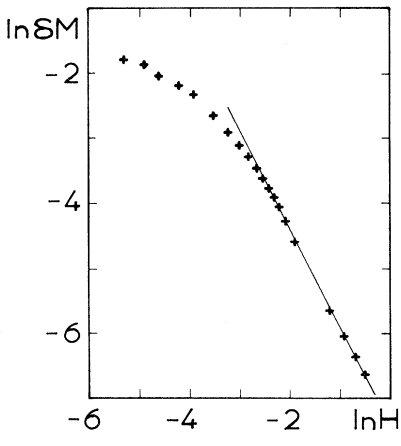

FIG. 7. Detail of magnetization curve, $D=0.1$. The slope of the straight line is -1.54.

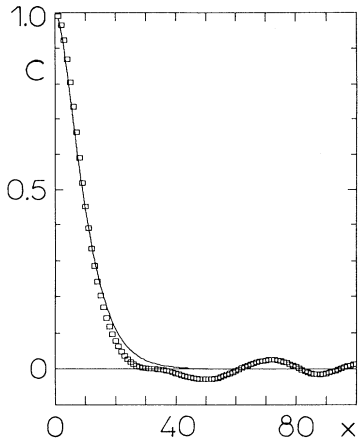

FIG. 8. Spin-spin correlation function $C(x)$ for $D=0.05$, $H=0$. The smooth curve is given by Eq. (13), with $k=0.187$, as determined by a least-squares fit to the first 20 data points.

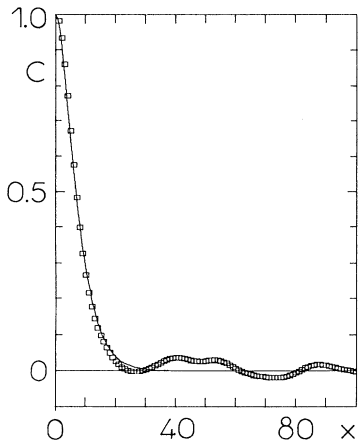

FIG. 9. Same as Fig. 8, but $D=0.1$ and $k=0.252$.

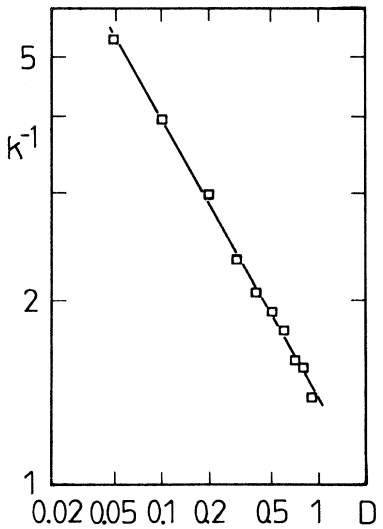

FIG. 10. Dependence of the correlation length, k^{-1}, on disorder strength D. The slope of the straight line is 0.46.

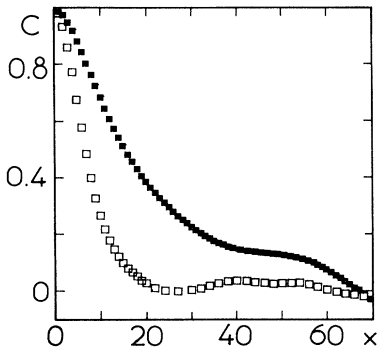

FIG. 11. Comparison of correlation functions at $H=0$ and $D=0.1$, after relaxing from a maximally disordered initial configuration (open squares), and from a smooth initial configuration (solid squares).

quacy of Imry-Ma type arguments, which focus on "typical" local energy minimum and thereby ignore the strong influence of the initial condition on the final state. (The same limitation of course applies to the calculation of the correlation function presented in the Appendix.) Evidence of the sensitivity of correlations to initial preparation is shown in Fig. 11, which contrasts the spin correlation function resulting from a smooth initial configuration with that obtained from the usual initial state of uncorrelated spins. The smooth configuration (obtained by averaging uncorrelated spins in blocks of five), evolves to a local energy minimum with a markedly greater correlation length.

E. Transverse correlation functions

In Sec. II B we presented a rather straightforward argument for the correlation of transverse spin com-

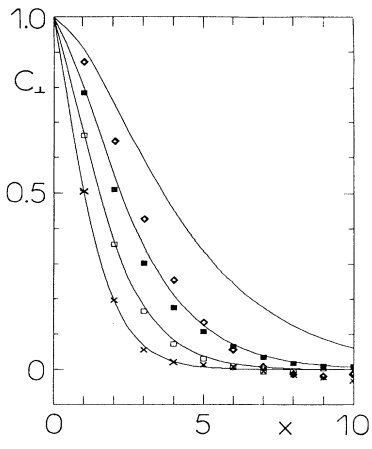

FIG. 12. Normalized transverse correlation function $C_\perp(x)$ for $D=0.5$ and $H=0.2$ (diamonds), $H=0.5$ (solid squares), $H=1.0$ (open squares), and $H=2.0$(×). The smooth curves are given by Eq. (11) with the prefactor set to unity.

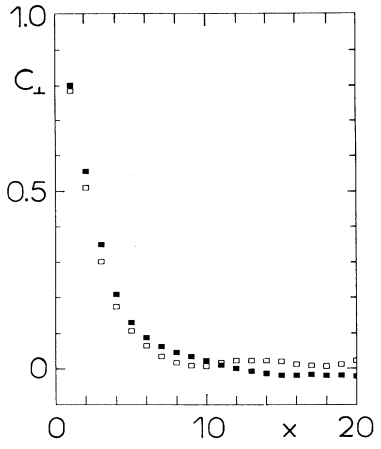

FIG. 13. Comparison of normalized transverse correlation functions for $H=0.5$ and $D=0.5$ (solid squares), and $D=0.1$ (open squares).

ponents, under the assumption that the external field is sufficiently strong that the θ_i are typically small. In Fig. 12 we compare *normalized* transverse correlation functions observed in simulations (averaged over five independent samples) with the theoretical prediction. [The latter is given by Eq. (11), ignoring the prefactor.] Note that in this case the correlation length Q is not treated as an adjustable parameter. Good agreement between theory and simulation is observed for $D=0.5$ and $H=2.0$, 1.0, and 0.5, corresponding to $M=0.9939$, 0.9831, and 0.9361, respectively. The agreement breaks down for $H=0.2$, where the assumption of a nearly magnetized system is no longer valid ($M=0.64$ in this case). The results shown in Fig. 13 support the prediction that the normalized transverse correlation function is independent of D.

F. Susceptibility

We determined the susceptibility for $D=0.05$, 0.1, 0.2, and 0.5 (averaging, in each case, over three independent samples) by measuring the change in magnetization in response to very weak fields ($-0.005 \le H \le 0.005$), following relaxation at $H=0$. (Typical "spontaneous" magnetizations of 0.01–0.02 are a finite-size effect.) As is shown in Fig. 14, the results are quite consistent with the prediction[5–7] $\chi \propto D^{-4/3}$.

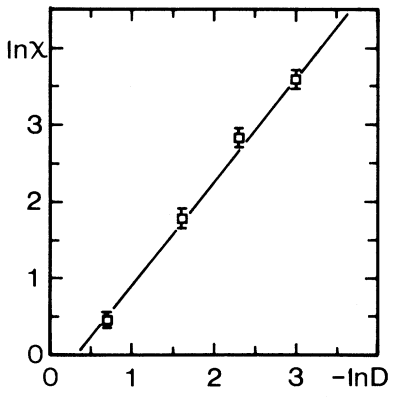

FIG. 14. Dependence of the magnetic susceptibility (in zero field) on disorder D. The slope of the straight line is 4/3.

V. DISCUSSION

Our simulations of the random-anisotropy model in one dimension, at zero temperature, suggest that the model must be understood from a dynamic, nonequilibrium vantage. We have shown that hysteresis persists even for very weak disorder, i.e., $D=0.1$. This confirms the result of Serota and Lee[18] who found significant hysteresis for $D/J=0.5$. Further evidence of the importance of nonequilibrium effects is our finding that correlations depend strongly upon the initial condition. Since qualitative features (e.g., hysteresis) are insensitive to details of the dynamics, we may expect nonergodic or glassy behavior in magnets with random anisotropy, evolving on laboratory time scales at low temperatures.

Several theoretical predictions—for some aspects of the magnetization curve, and for the scaling of the correlation length k^{-1} with disorder strength—are contradicted by simulation results. (We are not aware of any argument which explains the observed scaling, $k^{-1} \propto D^{0.46}$). On the other hand, predictions for the dependence of the susceptibility upon D, and for transverse correlations in a strong field, are confirmed rather nicely. A unified interpretation of the conflicts and agreements between theory and simulation is not obvious. Certain of our findings suggest a fundamental inadequacy in the usual static description. The presence of hysteresis, and the marked dependence of the correlations upon initial conditions point to the need for a dynamical theory.

While we believe that a more complete theory of the random-anisotropy model must incorporate memory effects, it is also clear that some predictions of the static approach are correct. Theory and simulation are in accord concerning the transverse correlation function, and the magnetization, both in a strong field. In these cases the $\mathbf{H}\cdot\mathbf{S}$ term dominates the energy, forcing the system into a rather well-defined low-energy state. (There may still be a number of local energy minima, accessible from various initial configurations, but their properties are more uniform, being determined primarily by the external field.) Here disorder comprises a perturbation whose effects may be accounted for in a simple manner. The susceptibility, in contrast, has been determined in the *absence of an external field,* and so the confirmation of the (essentially static) prediction,[5–7] $\chi \propto D^{-4/3}$ is noteworthy. It would be interesting to know whether the susceptibility depends upon the initial state of the system.

There are several directions for future work on the random-anisotropy model. It will be of interest to study hysteresis and other dynamic aspects in greater detail, as well as the effects of finite temperature, in simulations. We expect the hybrid algorithm introduced in this paper to permit more extensive studies of the weak-disorder re-

gime. Finally, we note that our considerations may be relevant to chain spin systems with an easy-plane anisotropy, such as $CsNiF_3$ and $(C_6H_{11}NH_3)CuBr_3$ (Refs. 21 and 22), in the presence of random fields or anisotropies.

ACKNOWLEDGMENTS

We are grateful to George Stell, Bernard Derrida, and Bernard Barbara for helpful discussions. We also thank Mr. E. Gan for his assistance with some of the initial simulations. The simulations were performed on the facilities of the University Computing Center of the City University of New York. This work was supported in part by PSC-CUNY Grant Number 661378.

APPENDIX: CORRELATION FUNCTION IN THE MEAN-SPHERICAL APPROXIMATION

Consider the energy functional Eq. (2), but with the fixed spin modulus condition $|\mathbf{S}_i|=1$ replaced with $\langle \mathbf{S}^2\rangle=1$ (i.e., the *mean-spherical approximation).* Our problem is to minimize the functional:

$$E'=\int dx\left[\frac{\alpha}{2}(d\mathbf{S}/dx)^2-\frac{\beta}{2}(\hat{\mathbf{n}}\cdot\mathbf{S})^2\right]-\lambda\int dx\,\mathbf{S}^2\ , \tag{A1}$$

where λ is a (constant) Lagrange multiplier. Extremal configurations $\mathbf{S}(x)$ satisfy

$$\alpha\, d^2\mathbf{S}/dx^2+\beta\hat{\mathbf{n}}(\hat{\mathbf{n}}\cdot\mathbf{S})+2\lambda\mathbf{S}=0 \tag{A2}$$

or

$$(d^2/dx^2-k^2)\mathbf{S}=-\frac{\beta}{\alpha}\hat{\mathbf{n}}(\hat{\mathbf{n}}\cdot\mathbf{S})\ , \tag{A3}$$

where we put $\lambda=-\alpha k^2/2$ $(k^2>0)$. The formal solution of Eq. (A3) is

$$\mathbf{S}(x)=-\frac{\beta}{\alpha}\int dx'\,G_k(x-x')\hat{\mathbf{n}}'(\hat{\mathbf{n}}'\cdot\mathbf{S}')\ , \tag{A4}$$

where $\hat{\mathbf{n}}'=\hat{\mathbf{n}}(x')$ and similarly for $\mathbf{S}'$, and where the Green's function is

$$G_k(x)=-\frac{1}{2k}e^{-k|x|}\ . \tag{A5}$$

From Eq. (A4) we have a formal expression for the correlation function:

$$\langle \mathbf{S}(x_1)\cdot\mathbf{S}(x_2)\rangle=\left[\frac{\beta}{\alpha}\right]^2\int dx'\int dx''\,G_k(x_1-x')G_k(x_2-x'')\langle\hat{\mathbf{n}}'\cdot\hat{\mathbf{n}}''n_\parallel' n_\parallel'' S'S''\rangle\ , \tag{A6}$$

where $n_\parallel(x)$ is the component of $\hat{\mathbf{n}}(x)$ along $\mathbf{S}(x)$. Now for weak anisotropy, $\mathbf{S}(x)$ is only weakly correlated with $\hat{\mathbf{n}}(x)$, and we may replace $\langle\hat{\mathbf{n}}'\cdot\hat{\mathbf{n}}''n_\parallel' n_\parallel'' S'S''\rangle$ with $\langle\hat{\mathbf{n}}'\cdot\hat{\mathbf{n}}''n_\parallel' n_\parallel''\rangle\langle S'S''\rangle$. The easy axes $\hat{\mathbf{n}}(x)$ have only short-range correlations, so that

$$\langle\hat{\mathbf{n}}'\cdot\hat{\mathbf{n}}''n_\parallel' n_\parallel''\rangle=\tfrac{1}{2}\Gamma(|x'-x''|)\ , \tag{A7}$$

where $\Gamma(0)=1$ and $\Gamma(x)\to 0$ for $|x|\gg a$, where a is the correlation length for the easy axes. (In the discrete model, a is one lattice spacing.) The correlation length for $\mathbf{S}(x)$ is k^{-1}, and in the weak-anisotropy limit we expect that $a\ll k^{-1}$. The coefficient in Eq. (A7) is found by evaluating the lhs at $x'=x''$; it gives $\langle n^2 n_\parallel^2\rangle=\langle n_\parallel^2\rangle=\langle\cos^2\theta\rangle=1/2$. Using Eq. (A7) in Eq. (A6), and replacing $\langle S'S''\rangle$ with $\langle(\mathbf{S}')^2\rangle=1$ (justified by the fact that $\mathbf{S}$ is correlated on a much longer scale than is $\hat{\mathbf{n}}$), we obtain

$$\langle \mathbf{S}(x_1)\cdot\mathbf{S}(x_2)\rangle=\left[\frac{\beta^2 r}{2\alpha^2}\right]\int dx\,G_k(x_1-x)G_k(x_2-x)\ , \tag{A8}$$

where $r\equiv\int dx\,\Gamma(x)\simeq a$. After performing the remaining integration, one finds

$$\langle \mathbf{S}(x_1)\cdot\mathbf{S}(x_2)\rangle=\frac{\beta r^2}{2\alpha^2}\frac{1}{4k^2}(k^{-1}+|x_1-x_2|)e^{-k|x_1-x_2|}\ . \tag{A9}$$

Setting $x_1=x_2$, and applying the condition $\langle\mathbf{S}^2\rangle=1$, we finally obtain Eqs. (13) and (14). For comparison with simulations of the lattice model, we set $\alpha=J,\beta=2D$, and $r=1$. Thus, in the mean-spherical approximation, local energy minima are characterized by a ferromagnetic correlation length $R_f=k^{-1}\propto(J/D)^{2/3}$. This is in accord with the prediction of the Imry-Ma argument for the correlation length in the *ground state.*

[1]R. Harris, M. Plischke, and M. J. Zuckerman, Phys. Rev. Lett. **31**, 160 (1973).
[2]See E. M. Chudnovsky, J. Appl. Phys. **64**, 5770 (1988) for a review, and Refs. 3 and 4 for the most recent experimental results.
[3]P. M. Gehring *et al.*, Phys. Rev. B **41**, 9134 (1990).
[4]J. Tejada *et al.*, Phys. Rev. B **42**, 858 (1990).
[5]E. M. Chudnovsky and R. A. Serota, Phys. Rev. B **26**, 2697 (1982); J. Phys. C **16**, 4181 (1983).
[6]V. S. Dotsenko and M. V. Feigelman, J. Phys. C **16**, L803 (1983).
[7]A. Aharony and E. Pytte, Phys. Rev. B **27**, 5872 (1983).
[8]E. M. Chudnovsky, W. M. Saslow, and R. A. Serota, Phys. Rev. B **33**, 251 (1986).
[9]Y. Imry and S. K. Ma, Phys. Rev. Lett. **35**, 1399 (1975).
[10]E. Callen, Y. I. Liu, and J. R. Cullen, Phys. Rev. B **16**, 263 (1977).
[11]R. A. Pelcovits, E. Pytte, and J. Rudnick, Phys. Rev. Lett. **40**,

476 (1978); R. A. Pelcovits, Phys. Rev. B **15**, 465 (1979).
[12]R. Alben, J. J. Becker, and M. C. Chi, J. Appl. Phys. **49**, 1653 (1978).
[13]K. H. Fisher and A. Zippelius, J. Phys. C **18**, L1135 (1985).
[14]W. M. Saslow, Phys. Rev. B **35**, 3454 (1987).
[15]R. Fisch, Phys. Rev. B **35**, 873 (1989); **42**, 540 (1990).
[16]E. M. Chudnovsky, J. Magn. Magn. Mater. **79**, 127 (1985).
[17]B. Derrida and A. Zippelius, J. Phys. (Paris) **47**, 955 (1986).
[18]R. A. Serota and P. A. Lee, Phys. Rev. B **34**, 1806 (1986); J. Appl. Phys. **61**, 3965 (1987).
[19]B. Dieny and B. Barbara, Phys. Rev. B **41**, 11 549 (1990).
[20]B. Barbara and B. Dieny, Physica **130B**, 245 (1985).
[21]A. P. Ramirez and W. P. Wolf, Phys. Rev. Lett. **49**, 227 (1982).
[22]A. M. C. Tinus, W. J. M. de Jonge, and K. Kopinga, Phys. Rev. B **32**, 3154 (1985).